

Techno-Economic Analysis of Hybrid Battery-Hydrogen Storage System for Passive and Conventional Residential Buildings [#]

Tageui Hong ¹, Seungho Shin ¹, Yeonsook Heo ^{1*}

1 School of Civil, Environmental and Architectural Engineering, Korea University, 145 Anam-ro, Seongbuk-gu, Seoul, Republic of Korea

(Corresponding Author: yeonsookheo@korea.ac.kr)

ABSTRACT

This study investigates the techno-economic performance of hybrid renewable energy systems integrating PV, battery storage, and green hydrogen storage for conventional and passive residential buildings. Using TRNSYS simulations, parametric cases were evaluated to explore cost–self-sufficiency trade-offs across three system configurations: PV-only, PV-Battery, and PV-Battery-Hydrogen. Pareto-optimal solutions were identified based on self-sufficiency ratio (SSR) and annualized system cost. The results showed that incorporating hydrogen systems significantly improved SSR with modest incremental system cost relative to battery-only systems. Although high SSR was achievable with battery storage alone, it required extremely large capacities and costs. In the knee-point analysis, passive buildings—due to higher surplus energy—reduced long-term storage needs, enabling hydrogen system downsizing and achieving 97.2% SSR at lower annualized cost than the conventional buildings (80.3% SSR). These findings underscore that adopting hydrogen systems enables economically viable pathways to high energy self-sufficiency, with passive design further enhancing performance while minimizing system costs in residential buildings.

Keywords: hybrid energy system, hydrogen storage, battery energy storage system, passive residential building, TRNSYS simulation, techno-economic analysis

NOMENCLATURE

Abbreviations

PV	Photovoltaic
GSHP	Ground-Source Heat Pump
BESS	Battery Energy Storage System
FC	Fuel Cell
H ₂ T	Hydrogen Storage Tank

ELE	Electrolyzer
HT	Heat Tank (Hot-Water Thermal Tank)
SSR	Self-Sufficiency Ratio

1. INTRODUCTION

The urgency of climate change and the global transition toward carbon neutrality have intensified the demand for energy self-sufficient residential solutions [1]. The building sector accounts for a significant share of global energy consumption, making the development of net-zero energy buildings (NZEBS) essential to reducing operational emissions [2]. However, even in NZEBs, aligning intermittent renewable generation with time-varying demand remains a major challenge, particularly due to diurnal and seasonal mismatches [3,4].

Hybrid renewable energy systems (HRES) that integrate battery storage and hydrogen storage, including electrolyzer, hydrogen tanks, and fuel cells, mitigate these mismatches by storing surplus renewable energy [3,5]. Hydrogen storage is particularly effective for seasonal balancing due to its high energy density and long-term storage efficiency [6]. The performance and economic viability of such hybrid systems depend strongly on building energy demand profiles, which vary with load magnitude, temporal patterns, and seasonal imbalance [7]. Passive design strategies, such as enhanced insulation and airtightness, can reduce space conditioning loads, lower seasonal energy deficits, and increase surplus electricity available for storage [8]. However, most previous studies have optimized battery-hydrogen systems using fixed load profiles from conventional residential buildings, without considering how passive design measures affect storage sizing and overall system performance [9,10]. Consequently, few studies have compared how load profile differences between passive and conventional buildings influence

[#] This is a paper for the 11th Applied Energy Symposium: Low Carbon Cities & Urban Energy Systems (CUE2025), July 18-22, 2025, Kitakyushu, Japan.

hybrid storage system design, especially regarding long-term storage needs.

This study evaluates the techno-economic performance of hybrid PV-Battery-Hydrogen systems in both conventional and passive residential buildings using one-year TRNSYS simulations. We analyze the self-sufficiency ratio (SSR) and annualized system costs across storage configurations, considering variations in battery capacity, hydrogen system sizing, and their combined operation. Furthermore, we examine how passive design influences demand profiles and long-term storage needs. Through pareto front and knee point analyses, this study analyzes optimal storage configurations that balance system cost and self-sufficiency given the distinct demand characteristics of conventional and passive residential buildings. Our analysis quantifies how storage configuration and the passive strategies jointly shape techno-economic performance.

2. MATERIAL AND METHODS

2.1 Research framework

Fig.1 illustrates the research framework for evaluating hybrid PV-Battery-Hydrogen systems in residential buildings. The analysis compared two building types—a standard and a passive model—designed to reflect differing demand characteristics. The hybrid systems consist of PV, GSHP, HT, BESS, and hydrogen systems that include FC (PEMFC), ELE, and H₂T. Heat loads, including space heating and domestic hot water (DHW), were fully electrified using GSHP+HT, and their electricity consumption, including auxiliary components, was added to the total electric load to enable integrated annual energy assessment under a unified electricity-based framework. Heating systems were pre-sized to meet at least 95% of the annual heat demand. PV capacity was sized to satisfy an annual net-zero electricity balance in the standard residential building and then uniformly applied to both building types to ensure a common generation baseline. This uniform PV sizing established a controlled generation baseline to isolate passive-design effects; the larger surplus in the passive case is by design for storage evaluation.

Battery and hydrogen system capacities were treated as design variables. To facilitate comparative analysis, three representative system configurations were defined based on the inclusion of storage components: PV-only (Base Case), PV with battery storage (Case 1), and PV with both battery and hydrogen systems (Case 2). A simple rule-based operation strategy

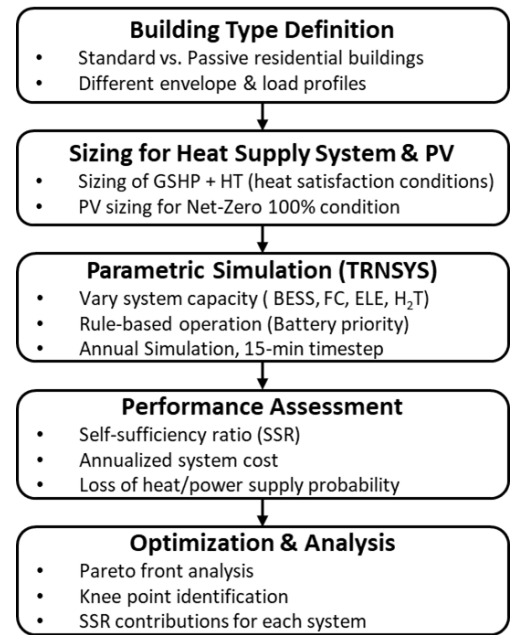


Fig. 1 Research framework diagram

prioritized the battery before hydrogen utilization. Using TRNSYS, parametric simulations were performed by combinations of the capacities of battery and hydrogen systems. Based on simulation results, each system configuration was evaluated based on key performance indicators. Pareto front analysis identified non-dominated solutions representing optimal trade-offs between SSR and cost. Knee point analysis compared cost-effective combinations between two different building types to examine the internal energy flows.

2.2 Rule-based operation logic

System operation followed a simple rule-based strategy that prioritized the battery and utilized hydrogen storage as a secondary buffer for surplus and deficit conditions. During PV surplus, electricity was first charged to the battery up to 90% state-of-charge (SOC). Any remaining excess was then sent to the ELE for hydrogen production and stored in the H₂T. To avoid part-load inefficiency, the ELE was not operated when surplus power was below 25% of its rated capacity, in which case the surplus was exported to the grid. Only the operational electricity required by the hydrogen compressor was assumed to come from the grid. When demand exceeded available PV power, the battery discharged down to 20% SOC first. If additional power was required, the FC operated in load-following mode to convert stored hydrogen to electricity until the H₂T reached 10% H₂T level. During FC operation, by-product heat was recovered to the HT and contributed to meet heat load. If supply still fell short, the residual load was met by grid import. Conversely, if surplus electricity

remained after both battery and hydrogen storage reached their upper limits, it was exported to the grid.

2.3 Performance index

System performance is evaluated using the self-sufficiency ratio (SSR) and the annualized system cost. These indices indicate the degree of renewable-based energy autonomy and grid independence, and the capital burden associated with a given configuration. SSR is defined as the share of total annual electricity demand met without grid imports. Energy that originates from on-site PV is credited, whether supplied directly to the load or discharged later from storage systems.

Annualized system cost is the sum of annualized capital charges with O&M allowance for all systems. For each system, capacity is multiplied by its unit capital price considering a component-specific lifespan from [3,9]. These annual charges are summed across components for each system configuration. Electricity purchase tariffs, export revenues, taxes, and incentives are excluded from the cost boundary in this study.

3. CASE DESCRIPTION

3.1 TRNSYS simulations

TRNSYS simulation was employed to generate energy demand profiles for both buildings, and pre-size PV, GSHP, and HT first. In addition, parametric simulations were conducted by varying the capacities of BESS, FC, ELE, and H₂T. Each configuration was simulated for one year at a 15-minute timestep to capture both seasonal and diurnal variability in load and generation. All simulations started in March to reflect the seasonal sequence of surplus accumulation in warmer months and thermal demand coverage in winter.

Additional boundary conditions and system operations were as follows. HT started at 45°C and acted as a thermal buffer. GSHP operated in 5 kW stages, turning on at HT<50°C, reducing stages above 60°C, and holding between 50-60°C. The FC used five part-load levels (0, 0.25, 0.50, 0.75, 1.00), turning on under power deficit and stepping down one level per surplus interval. Initial storage states were battery SOC = 20% and H₂T level = 10%. The parametric design increments were HT 1 m³, GSHP 5 kW, FC 5 kW, H₂T 5 m³, and ELE 26 kW. Battery was stepped by 5 kWh at small sizes, by 100 kWh at >500 kWh, and by 500 kWh at >5,000 kWh.

3.2 Building modeling

Two residential building types were modeled: (1) a standard building reflecting typical Korean apartment specifications, and (2) a passive building with improved

Table 1 Envelope specifications between standard and passive residential buildings

Component	Param.	Unit	Standard	Passive
Window	U-value	W/m ² K	2.10	0.80
	SHGC	-	0.80	0.52
Exterior wall	U-value	W/m ² K	0.35	0.15
Roof	U-value	W/m ² K	0.18	0.15
Infiltration	ACH	1/hr	0.5	0.12

thermal envelope performance. The standard model was based on a simplified reference apartment from Jung et al. [11], with thermal properties derived from a national database of Korean apartment buildings. Building geometry was created in SketchUp and imported into TRNBuild software. Heating and cooling setpoints were set to 20 °C and 26 °C, respectively. The passive building adopted enhanced envelope specifications, including lower U-values and reduced infiltration rates, as summarized in Table 1.

Hourly plug-in load and thermal load profiles were generated using empirical data and building simulations, respectively. Space heating and cooling loads were simulated in TRNSYS using a typical meteorological year (TMY) dataset for Seoul. Cooling demand was converted to electricity, assuming a coefficient of performance (COP) of 3.0. All load profiles were scaled to five-story apartment, providing full-year power and thermal demand inputs for simulations of hybrid energy systems.

3.3 Thermal supply systems and PV pre-sizing for hybrid storage optimization

To ensure the electricity-based evaluation framework, the thermal supply (GSHP, HT) and PV systems were pre-sized for each building case. Thermal supply systems were sized first to ensure reliable heat supply and to establish an electrified thermal load for subsequent design of power supply and storage systems. The GSHP and HT capacities were determined through separate sizing simulations to satisfy at least 95% annual heat demand. As a result, thermal demand was met using a 20 kW GSHP and 1 m³ HT for the standard case, and a 10 kW GSHP and 1 m³ HT for the passive case. The electrification of thermal load was applied through the operation of a sized GSHP system and circular pumps. The corresponding electricity consumption was included in the total power demand and fully reflected in sizing the PV-battery-hydrogen system. Subsequently, a 35 kW PV system, sized to meet the annual net-zero condition in the standard building for base case, was uniformly applied to both building types to ensure identical PV generation (54,371 kWh/year).

3.4 Electrified building demand analysis

Fig.2 illustrates the monthly energy surplus and deficit patterns for the two building types, derived from 15-minute simulation data aggregated into hourly energy (kWh). Positive values represent PV surplus energy, typically generated during daytime hours, while negative values represent electricity deficits, which generally occur during evening and nighttime hours. Even in the PV-only baseline, each month contains both surplus and deficit hours, indicating a persistent diurnal (day–night) mismatch between PV generation and demand. The monthly PV-based energy balance showed differences between the standard and passive buildings particularly during the cold season (January–March and November–December).

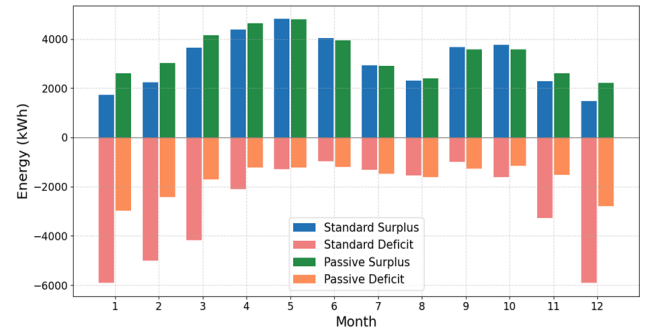


Fig. 2 Monthly surplus and deficit energy from PV generation

Both buildings exhibited large surpluses during summer and mid-season months from April to October. In the standard residential building, substantial power deficits occurred from November to March. These deficits peak in January and February, where total shortfalls exceeded over 70% of total demand due to elevated heating loads and reduced PV generation. This seasonal mismatch necessitates long-term energy storage. In contrast, the passive building maintained a more balanced annual profile, with minimal deficits during winter due to reduced overall demand from the passive design.

three cases: (1) Base Case: PV only (S0, P0), (2) Case 1: PV-battery (S1, P1), and (3) Case 2: PV-battery-hydrogen system (S2, P2).

In both building types, adding a small-capacity battery to PV increased SSR with only a small increase in cost. Further inclusion of hydrogen systems led to significantly higher SSR improvements, with increases of >18.2% (standard) and >16.4% (passive) versus battery-only configurations (Case 1). This highlights the hydrogen system’s role for addressing seasonal mismatches beyond the diurnal balancing from the battery. These sequential additions formed a steep, cost-effective segment of the pareto front in the low-cost region. In Case 2, beyond a threshold investment level, additional system cost increases yielded only marginal improvements in SSR. This flattening trend was primarily attributed to excessive battery sizing, whereas the capacities of hydrogen system components (FC, ELE, H₂T) remained nearly unchanged in both building types.

4. RESULTS

4.1 Pareto-optimal configurations

Fig.3 illustrates the pareto-optimal samples for analyzing system configurations between SSR and annualized system cost in standard and passive buildings. Out of 34,155 simulation runs, 89 pareto-optimal points were identified for the standard building and 87 for the passive building. Selected points were categorized as

In the standard building, Base case (S0) was a single sample with an SSR of 33.0% and an annual cost of around \$3,200. In Case 1 (S1), the highest SSR reaches only 51.7%, indicating that battery systems are insufficient for achieving high SSR in standard residential building. Most pareto-optimal samples (80 samples)

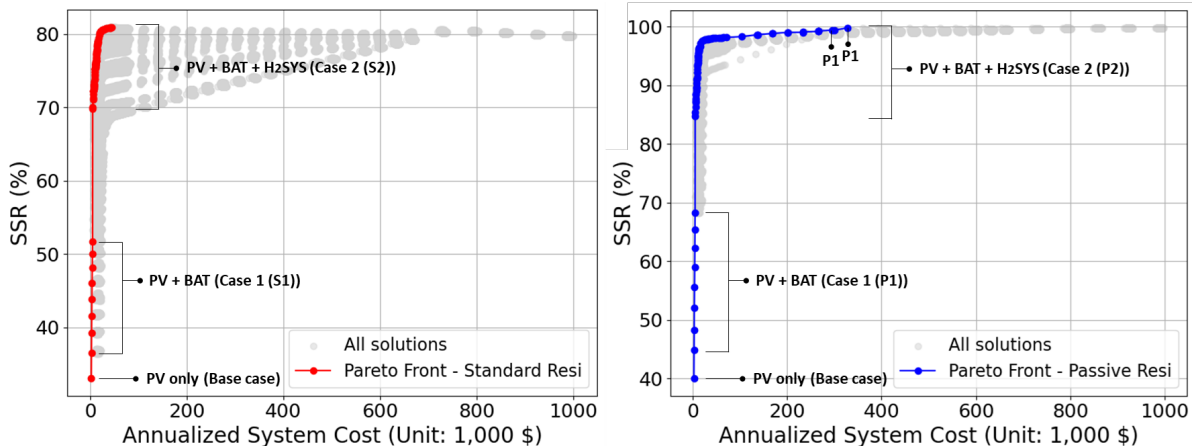


Fig. 3 Pareto front samples for residential building types: Annualized system cost vs. Self-sufficiency ratio

were found in Case 2 (S2), where hydrogen systems were integrated. In this group, SSR values ranged from 69.9% to 80.9%, with annual system costs between approximately \$7,000 and \$46,000.

For the passive building, a PV-only case (P0) showed an SSR of 40.1%. Due to the halved GSHP capacity, the annualized system cost was reduced to approximately \$1,760. In Case 1 (P1), ten samples were observed. Among them, two samples had disproportionately large battery capacities (4,500 and 5,000 kWh), with sharply increased costs—reaching up to \$328,100—thus forming a group of outliers. Therefore, the P1 group was divided into a low-cost/mid-SSR cluster (SSR 44.9–68.3%) and a high-cost cluster. In Case 2 (P2), 76 pareto-optimal samples were identified, with SSRs ranging from 84.7% to 99.4% and costs spanning from \$5,600 to \$300,600, forming a much broader cost–self-sufficiency spectrum.

From a building design strategy perspective, passive buildings consistently exhibited higher SSR values compared to standard buildings across all cases. This advantage results primarily from load reductions achieved through passive design strategies. Passive buildings approached nearly 100% SSR, underscoring that both demand-side (passive design) and supply-side (hybrid storage) strategies are essential for achieving cost-efficient grid independence. Importantly, while battery-only systems can theoretically achieve high SSRs, doing so requires disproportionately large battery capacities and leads to significantly higher system costs.

4.2 Knee point analysis

Based on the filtered pareto-optimal samples, knee point analysis was conducted for both the standard (S2) and passive (P2) residential buildings. Fig. 4 shows the Case 2 pareto fronts with knee points for both buildings. The knee point was identified by the largest deviation from the straight line between the two extreme points on the normalized cost-SSR pareto front. The S2 knee point achieved an SSR of 80.3% at an annualized system cost of approximately \$20,140. The corresponding system consisted of 150 kWh battery, 30 kW FC, 26 kW ELE, and 20 m³ H₂T. In contrast, the P2 knee point achieved a substantially higher SSR of 97.2% at a lower annualized cost of \$15,917. Despite having the same battery capacity (150 kWh), the hydrogen systems in P2 were significantly downsized to 10 kW FC, 26 kW ELE, and 10 m³ H₂T. As a result, the passive building approached near-complete energy self-sufficiency at a lower cost.

Fig. 5 presents the energy supply breakdown for the knee-points. It compares how each system contributes to meeting the demand (supply energy shown as

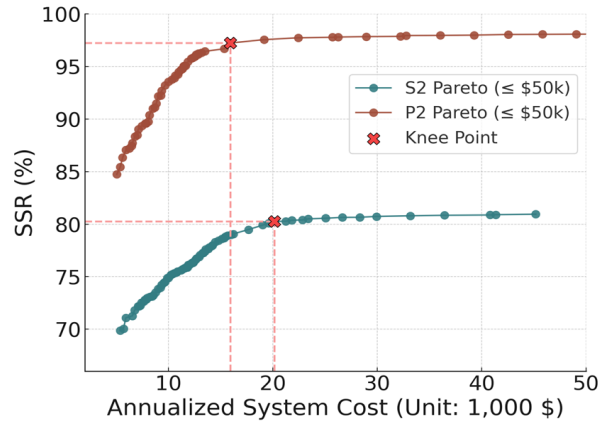


Fig. 4 Pareto fronts for Case 2 (Battery+H₂ systems)

positive) and how surplus electricity is exported to the grid (export shown as negative) in standard and passive buildings. The passive building had a total annual demand of 42,171 kWh, while standard building showed higher total demand (63,691 kWh) due to heating-season loads (see Fig. 2). In the passive building, PV generation directly supplied 21,704 kWh (51.4%), the 150 kWh battery delivered 17,523 kWh (41.6%), and FC supplied 1,860 kWh (4.4%) using stored hydrogen. Grid imports accounted for only 1,083 kWh (2.6%), achieving 97.2% SSR. In contrast, the standard building, despite a larger direct PV supply (30,175 kWh, 47.4%) and a similar battery supply (17,665 kWh, 27.9%), required more hydrogen support (3,315 kWh, 5.2%) and relied more heavily on grid imports (12,436 kWh, 19.5%).

As an additional analysis, grid export and the associated potential revenue were quantified alongside

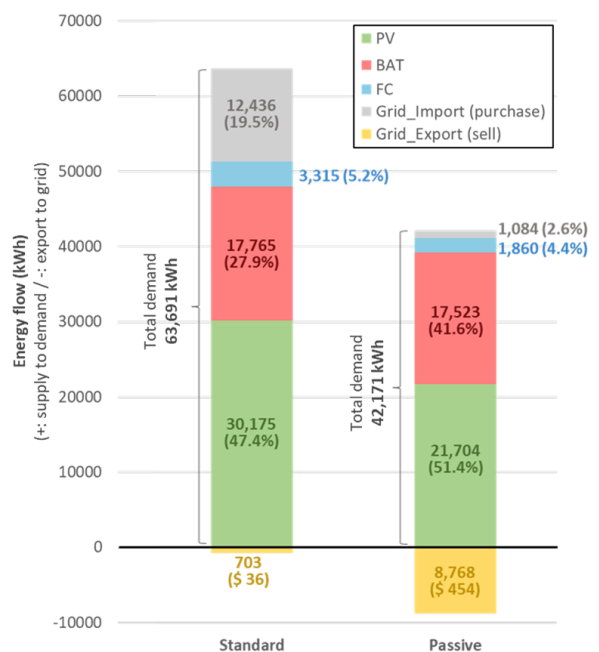


Fig. 5 Demand coverage by system components and grid export at selected knee points

grid import to understand power-flow dynamics in Fig. 5. Although grid exports are excluded from the annualized system cost, it explained annual PV-to-grid interaction and suggests additional economic benefits beyond the defined cost boundary. Passive building exported 8,768 kWh/year of surplus electricity to the grid after fully charging the battery and partially converting surplus to hydrogen, generating 454 USD/year of revenue, while the standard building exported only 703 kWh/year with minimal revenue (36 USD/year) and remained dependent on costly grid imports to meet deficits.

Although passive buildings generated more PV surplus due to reduced demand, long-term storage requirements were significantly reduced. These lower seasonal deficits allowed surplus electricity to be exported without oversizing the hydrogen system capacity, enabling downsized system configuration observed at the P2 knee point. Conversely, standard building required a larger hydrogen system to compensate for seasonal mismatches. These results indicate that passive design reduces seasonal storage requirements and enables the hydrogen system to be minimized, achieving near-complete energy self-sufficiency at lower system cost.

5. CONCLUSIONS

This study evaluated hybrid PV-Battery-Hydrogen systems in conventional and passive residential buildings using TRNSYS simulations. Pareto front and knee point analyses identified cost-effective system configurations that maximize the SSR. The results show that battery storage alone cannot economically achieve high SSR, whereas hybrid storage systems significantly improve SSR by providing a long-term energy buffer. In passive buildings, reduced seasonal demand lowers long-term storage requirements, allowing battery storage to manage most daily fluctuations and enabling downsizing of hydrogen systems to address minimal remaining energy imbalances. These findings highlight the importance of considering passive design with optimized hybrid storage to improve both energy autonomy and economic feasibility. Future work should incorporate additional performance indicators, such as grid interaction metrics, and extend the analysis to buildings with different demand profiles to support applicability of hybrid energy strategies across diverse building types.

ACKNOWLEDGEMENT

This work was supported by the National Research Foundation of Korea (NRF) grant funded by the Korea government (MSIT) (No. 2020R1A5A1018153).

REFERENCES

- [1] Naseri, N., El Hani, S., Machmoum, M., Elbouchikhi, E., & Daghour, A. (2024). Energy Management Strategy for a Net Zero Emission Islanded Photovoltaic Microgrid-Based Green Hydrogen System. *Energies*, 17(9), 2111.
- [2] Mobayen, S., Assareh, E., Izadyar, N., Jamei, E., Ahmadinejad, M., Ghasemi, A., ... & Pak, W. (2025). Multi-functional hybrid energy system for zero-energy residential buildings: Integrating hydrogen production and renewable energy solutions. *International Journal of Hydrogen Energy*, 102, 647-672.
- [3] Go, J., Byun, J., Orehounig, K., & Heo, Y. (2023). Battery-H₂ storage system for self-sufficiency in residential buildings under different electric heating system scenarios. *Applied Energy*, 337, 120742.
- [4] Zhang, Y., Lundblad, A., Campana, P. E., & Yan, J. (2016). Comparative study of battery storage and hydrogen storage to increase photovoltaic self-sufficiency in a residential building of Sweden. *Energy Procedia*, 103, 268-273.
- [5] Liu, J., Chen, X., Yang, H., & Shan, K. (2021). Hybrid renewable energy applications in zero-energy buildings and communities integrating battery and hydrogen vehicle storage. *Applied Energy*, 290, 116733.
- [6] Yousri, D., Farag, H. E., Zeineldin, H., & El-Saadany, E. F. (2023). Integrated model for optimal energy management and demand response of microgrids considering hybrid hydrogen-battery storage systems. *Energy Conversion and Management*, 280, 116809.
- [7] Adeyemo, A. A., & Amusan, O. T. (2022). Modelling and multi-objective optimization of hybrid energy storage solution for photovoltaic powered off-grid net zero energy building. *Journal of Energy Storage*, 55, 105273.
- [8] Lindberg, K. B. (2017). Impact of Zero Energy Buildings on the Power System: a study of load profiles, flexibility and system investments.
- [9] Byun, J., Go, J., Kim, C., & Heo, Y. (2023). Reliability, economic, and environmental analysis of fuel-cell-based hybrid renewable energy networks for residential communities. *Energy Conversion and Management*, 284, 116964.
- [10] Byun, J., & Heo, Y. (2021, September). Design and analysis of a renewable energy network based on fuel cells in a residential community. In *Building Simulation 2021* (Vol. 17, pp. 3276-3283). IBPSA.
- [11] Jung, H. K., Jeong, Y. S., & Huh, J. H. (2017). A study on the establishment of reference buildings of apartments and estimation of energy consumption. *Journal of the Architectural Institute of Korea Planning & Design*, 33(9), 45-52.